JACS
JOURNAL OF THE AMERICAN CHEMICAL SOCIETY
Article
pubs.acs.org/JACS

Monodisperse Cylindrical Micelles and Block Comicelles of Controlled Length in Aqueous Media

Ali Nazemi,[†] Charlotte E. Boott,[†] David J. Lunn,[†] Jessica Gwyther,[†] Dominic W. Hayward,[†] Robert M. Richardson,[‡] Mitchell A. Winnik,[§] and Ian Manners*[,†]

[†]School of Chemistry, University of Bristol, Bristol BS8 1TS, United Kingdom
[‡]H. H. Wills Physics Laboratory, University of Bristol, Bristol BS8 1TL, United Kingdom
[§]Department of Chemistry, University of Toronto, Toronto, Ontario M5S 3H6, Canada

Supporting Information

ABSTRACT: Cylindrical block copolymer micelles have shown considerable promise in various fields of biomedical research. However, unlike spherical micelles and vesicles, control over their dimensions in biologically relevant solvents has posed a key challenge that potentially limits in depth studies and their optimization for applications. Here, we report the preparation of cylindrical micelles of length in the wide range of 70 nm to 1.10 μm in aqueous media with narrow length distributions (length polydispersities <1.10). In our approach, an amphiphilic linear-brush block copolymer, with high potential for functionalization, was synthesized based on poly(ferrocenyldimethylsilane)-*b*-poly(allyl glycidyl ether) (PFS-*b*-PAGE) decorated with triethylene glycol (TEG), abbreviated as PFS-*b*-(PEO-*g*-TEG). PFS-*b*-(PEO-*g*-TEG) cylindrical micelles of controlled length with low polydispersities were prepared in *N*,*N*-dimethylformamide using small seed initiators via living crystallization-driven self-assembly. Successful dispersion of these micelles into aqueous media was achieved by dialysis against deionized water. Furthermore, B−A−B amphiphilic triblock comicelles with PFS-*b*-poly(2-vinylpyridine) (P2VP) as hydrophobic "B" blocks and hydrophilic PFS-*b*-(PEO-*g*-TEG) "A" segments were prepared and their hierarchical self-assembly in aqueous media studied. It was found that superstructures formed are dependent on the length of the hydrophobic blocks. Quaternization of P2VP was shown to cause the disassembly of the superstructures, resulting in the first examples of water-soluble cylindrical multiblock comicelles. We also demonstrate the ability of the triblock comicelles with quaternized terminal segments to complex DNA and, thus, to potentially function as gene vectors.

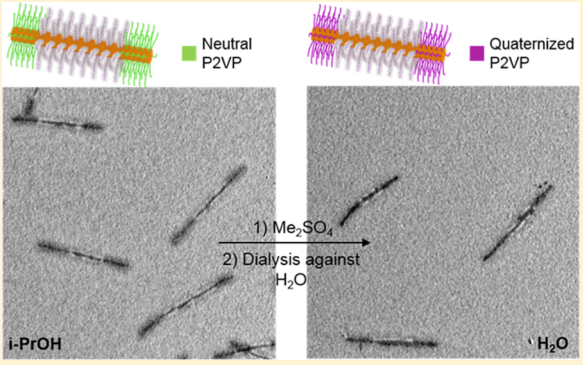

1. INTRODUCTION

Over the past few decades, block copolymer (BCP) nanoparticles have received considerable attention with respect to applications in biomedicine.[1−3] This interest partly stems from their higher thermodynamic and kinetic stabilities compared to assemblies obtained from low molecular weight surfactant analogues, which in turn results in their much higher critical aggregation concentrations.[4,5] In addition, the development of controlled living polymerization methods at the molecular level has enabled access to a diverse range of BCP assemblies.[6,7] Using solution-phase protocols, a wide range of morphologies including spherical and cylindrical micelles,[8] helical rods,[9] toroids,[10] macroscopic tubes,[11] and vesicles[12] have been obtained in solvents that are selective for one of the blocks. Such assemblies, in particular spherical micelles and vesicles, have been extensively explored for the encapsulation and delivery of a wide range of biomolecules including hydrophilic and hydrophobic drugs, proteins, oligonucleotides, and imaging agents.[13−15] The potential of such drug delivery vehicles in biomedicine is illustrated by the fact that they not only prolong the circulation time of their payloads and protect them from premature degradation, but can also be actively or passively targeted to desired tissues and organs.[16] This results in an increase of the bioavailability of a drug and a reduction of side effects. In this context, the shape, size, and rigidity of nanoparticulate therapeutic agents play a key role in determining their uptake efficiency, circulation time, and distribution in the body.[2] Although the optimal parameters vary according to the specific application, nonspherical structures such as one-dimensional (1D) particles appear to have a very promising role to play.[2,17−19] Specifically, it has been shown that blood circulation times of polydisperse BCP cylinders were longer than comparable spherical nanoparticles and the values increased with micelle length.[17] In addition, rod-like particles offer better cell uptake rates and extents in human melanoma cells compared to spherical particles.[20] Moreover, it has also been found that rod-like particles exhibit higher

Received: December 23, 2015
Published: March 22, 2016

DOI: 10.1021/jacs.5b13416
J. Am. Chem. Soc. 2016, 138, 4484−4493

Scheme 1. Synthesis of PFS-*b*-(PEO-*g*-TEG) BCP 4

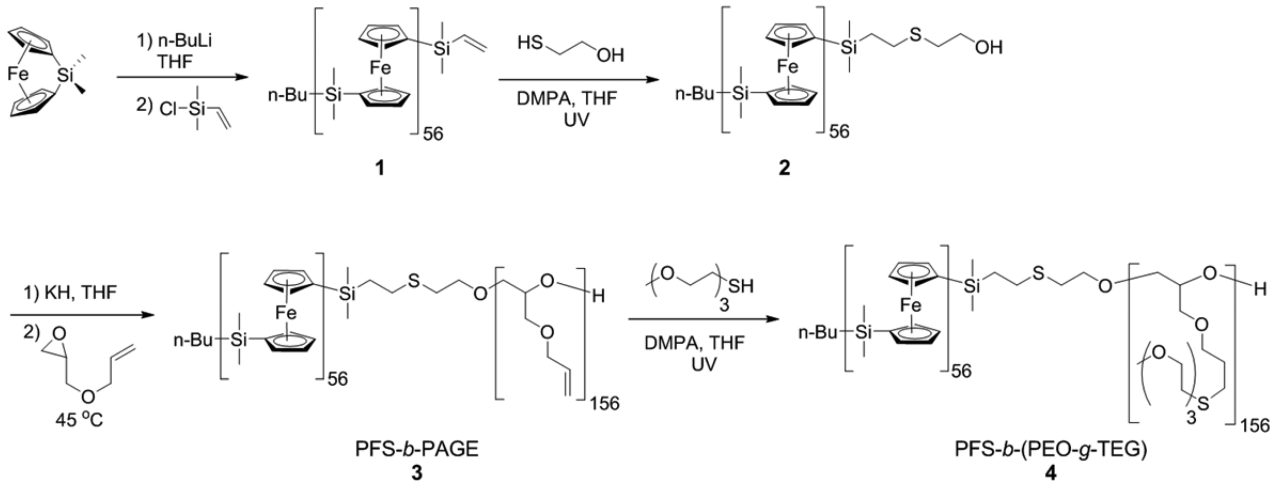

adhesion, which can be used as a means for targeting purposes of drug delivery vehicles to endothelium junctions.[21] Despite the great potential that cylindrical micelles offer in biomedical research, challenges with respect to their formation and, in particular, the lack of precise control over their dimensions, appear to represent a significant limitation.

Although near monodisperse cylindrical nanostructures can be obtained in the form of unimolecular micelles from bottle brush BCPs[22−24] and dendronized polymers,[25,26] time-consuming synthetic procedures are associated with the synthesis of the building blocks. Polydisperse cylindrical micelles can also be prepared from the self-assembly of BCPs with amorphous core-forming blocks in block selective solvents.[8,27] However, their formation is generally restricted to a small region of the compositional phase space and is often complicated by the coexistence of other morphologies.

The realization of well-defined cylindrical micelles with controlled lengths has recently been achieved in organic media by the self-assembly of BCPs with crystallizable core-forming blocks.[28] Core-crystallization appears to favor cylinder formation over a wide range of block ratios, but particularly in the case of long corona-forming blocks.[29] In this context, BCPs with crystallizable poly(ferrocenyldimethylsilane) (PFS),[30] polycaprolactone,[31,32] poly(L-lactic acid),[33,34] polyethylene,[35] polyacrylonitrile,[36] polythiophene,[37,38] and polyselenophene[39] core-forming blocks have been reported to form cylindrical micelles. By optimizing the self-assembly conditions, it is possible to achieve some control over the length of cylindrical micelles formed by a variety of poly(L-lactic acid)-[40−44] and polycaprolactone-based[45] BCPs in aqueous media. In addition, post-self-assembly methods such as fragmentation during extrusion have also been employed to reduce the length of cylindrical micelles.[17] However, to date, attempts to obtain near monodisperse cylinders with lengths that can be varied over a substantial range above ca. 300 nm that are dispersible in aqueous media using these approaches have been unsuccessful.

Using BCPs with crystallizable PFS core-forming blocks, our group has been able to access near monodisperse cylindrical micelles and block comicelles of controlled length in organic or fluorinated media in the range of 20 nm to several micrometers.[46,47] This has been achieved by sonication of the long polydisperse cylinders prepared by spontaneous nucleation in a selective solvent to form small seed micelles. Addition of molecularly dissolved BCP (unimer) then leads to growth from the seed termini. This process has been termed "living" crystallization-driven self-assembly (CDSA) as the cylinder length depends on the unimer to seed ratio, which is analogous to the behavior of a living covalent polymerization.[48] Furthermore, the addition of PFS BCP unimer with a different complementary block to that of the seed results in the formation of block comicelles, micelle analogues of BCPs.[48] Similar seeded growth approaches have also recently been reported for BCPs with other crystallizable core-forming blocks and also for π-stacking amphiphiles.[38,49−55] These developments have also provided access to new building blocks that allow the construction of a variety of complex hierarchical superstructures.[56−60]

Herein, in an attempt to tackle the above-mentioned limitations, we report the preparation of well-defined, water-soluble cylindrical micelles of controlled length over a broad range up to 1.10 μm, with the added advantage of having a readily functionalizable corona-forming block. Furthermore, we report the first example of the formation of water-soluble cylindrical block comicelles. In addition, the biorelevance of these cylindrical micelles was examined by investigating their binding ability to DNA.

2. RESULTS AND DISCUSSION

2.1. Synthesis and Characterization of Amphiphilic Linear-Brush BCP 4. To synthesize a suitable PFS-based amphiphilic BCP, we targeted a coblock that would be highly hydrophilic, biocompatible, and functionalizable for future applications. To achieve these properties, poly(allyl glycidyl ether) (PAGE) was chosen as the intermediate target. It can be synthesized via anionic polymerization methods on a large scale with narrow molecular weight distributions.[61] In addition, PAGE is an analogue of poly(ethylene oxide) with a high density of allyl groups along its backbone that can be readily functionalized.[62−64] This is particularly important because it opens up the possibility for the divergent preparation of a variety of BCPs for any targeted application with no need for protection−deprotection procedures. In fact, it has been shown that the allyl groups on PAGE backbone can be readily modified with biologically relevant molecules of interest via thiol−ene reactions.[65] On the basis of these features, PAGE-based materials have recently been used for hydrogel formation,[66] nanopatterning biomolecules,[67] drug delivery,[68−70] and lithium batteries.[71] In our approach, PFS_{56}-*b*-$PAGE_{156}$ (**3**)

DOI: 10.1021/jacs.5b13416
J. Am. Chem. Soc. 2016, 138, 4484−4493

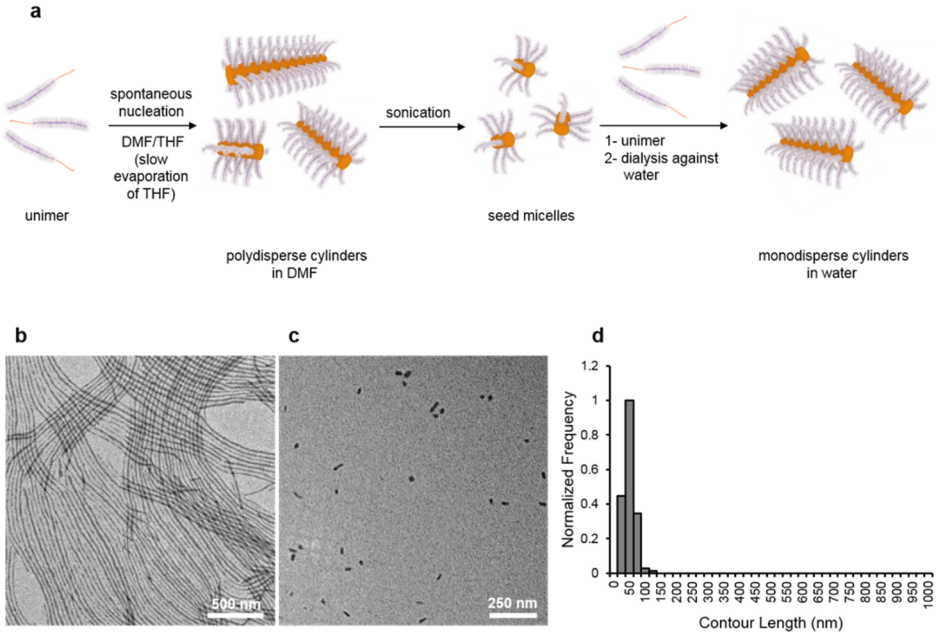

Figure 1. (a) Schematic representation of the preparation of near monodisperse cylinders in aqueous media; (b) TEM micrograph of long, polydisperse cylinders in DMF; (c) TEM micrograph of PFS-*b*-(PEO-*g*-TEG) seed micelles prepared by sonication of polydisperse cylinders; (d) Histogram of the contour length distribution of seeds in (c).

was first synthesized as an intermediate target. The synthetic procedure is shown in Scheme 1. A hydroxyl-terminated PFS homopolymer, **2**, was synthesized from a precursor (**1**) that was prepared by end-capping a living PFS polymer prepared by anionic polymerization,[72] using chlorodimethylvinylsilane. The vinyl end group was functionalized with 2-mercaptoethanol under photoinitiated thiol−ene "click" reaction conditions, using 2,2-dimethoxy-2-phenylacetophenone (DMPA), to quantitatively introduce a terminal alcohol.[73] The resulting hydroxyl-terminated PFS polymer, **2**, was then used as a macroinitiator for the anionic polymerization of allyl glycidyl ether (AGE) monomer. Potassium hydride (KH) was used as base for the deprotonation of the hydroxyl group in tetrahydrofuran (THF). The AGE monomer was then added and the resulting mixture was stirred at 45 °C for 16 h. The crude product was obtained in ca. 65−75% yield after precipitation of the reaction mixture into hexane. Purification by preparative size exclusion chromatography (SEC), to remove any uncapped PFS homopolymer and unreacted **2**, afforded the pure product **3** as an orange solid in ca. 20−35% yield with a low polydispersity index (PDI) of 1.20 (Figures S1). To impart additional hydrophilicity to the BCP, the vinyl groups of the PAGE block were then functionalized with thiol-terminated triethylene glycol (TEG) via the aforementioned photoinitiated thiol−ene reaction. The target linear-brush BCP **4** was readily purified by precipitation into hexane and was obtained as an orange gum in 71% yield with a PDI of 1.25 (Figures S1, S3, and S4). ^{1}H NMR analysis of PFS-*b*-(PEO-*g*-TEG) in CD_2Cl_2 confirmed the complete conversion of vinyl groups by disappearance of the peaks at δ = 5.91, 5.23, and 5.16 ppm, corresponding to vinyl groups, and emergence of new peaks at 2.69, 2.61, and 1.83 ppm corresponding to the thioether linkages formed (Figure S5 and Figure S6).

2.2. Self-Assembly of Amphiphilic Linear-Brush BCP, 4, to Form Cylindrical Micelles. Prior to exploring the linear-brush BCP **4**, the self-assembly behavior of the linear BCP **3** was investigated in polar, PAGE-selective organic solvents such as ethyl acetate (EtOAc) and *n*-butanol (*n*-BuOH). BCP **3** was dissolved in EtOAc and *n*-BuOH at 75 and 110 °C, respectively, for 10 min before being allowed to cool slowly to room temperature and aged for 2 days. Transmission electron microscopy (TEM) analysis of the drop-cast samples on carbon-coated copper grids revealed the formation of micrometer-long (>4 μm) cylinders in EtOAc (which were too long to measure accurately) and shorter analogues in *n*-BuOH (L_n = 497 nm, L_w = 637 nm, L_w/L_n = 1.28, σ/L_n = 0.53; L_n is number-average contour length, L_w is weight-average contour length, and σ is the standard deviation) (Figure S7).

With these promising results obtained for the intermediate polymer **3**, the self-assembly behavior of the amphiphilic linear-brush BCP **4** was then investigated. Initially, we targeted the direct self-assembly of the polymer in aqueous media. A THF solution of BCP **4** (10 mg/mL) was injected quickly into water to obtain a final polymer concentration of 0.5 mg/mL. TEM analysis of this sample at different time points revealed a very slow self-assembly process evidenced by the deposition of considerable amounts of film arising from remaining unimer (Figure S8). Small numbers of spherical micelles were initially formed, whereas mixtures of spheres, cylinders, and ill-defined 2D structures were present at later times. Cylindrical micelles were only exclusively observed after about 75 days (Figure S8). Similar results were obtained under a more thermodynamically controlled condition involving slow injection of water (0.95 mL, 15 μL/min) into a THF solution of **4** (10 mg/mL, 50 μL) (Figure S9) and also by heating samples to elevated temperatures (Figure S10). The slow nature of the cylinder formation and morphological transitions can be attributed to slow crystallization of the PFS-core in protic polar and hydrophilic solvents. A similar effect has been previously observed for PFS-*b*-poly(2-vinylpyridine) (P2VP) in ethanol.[74] As such a long period of time was undesirable for obtaining cylinders in water, we turned our attention to the self-assembly of **4** in water-miscible polar organic solvents. Initial attempts involved self-assembly of **4** in solvents such as methanol,

DOI: 10.1021/jacs.5b13416
J. Am. Chem. Soc. 2016, 138, 4484−4493

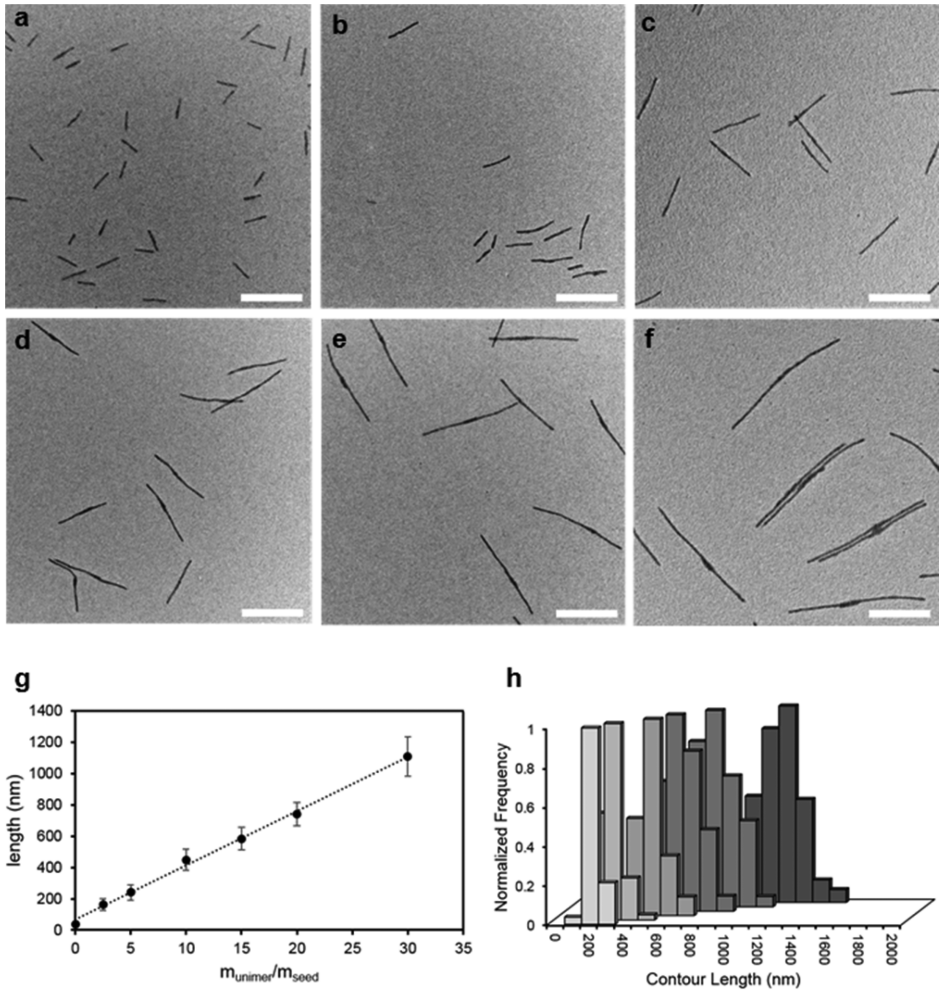

Figure 2. TEM micrographs of PFS-*b*-(PEO-*g*-TEG) cylindrical micelles, after dialysis into water, grown from PFS-*b*-(PEO-*g*-TEG) seed micelles (L_n = 38 nm) with m_{unimer}/m_{seed} of 2.5:1 (a), 5:1 (b), 10:1 (c), 15:1 (d), 20:1 (e), and 30:1 (f). Scale bars 500 nm. (g) Plot showing the linear dependence of cylinder length on m_{unimer}/m_{seed}. (h) Histograms showing the contour length distribution of cylindrical micelles with m_{unimer}/m_{seed} of 2.5:1, 5:1, 10:1, 15:1, 20:1, and 30:1 (front-back, respectively). These results are only illustrative of the control obtained. For example, low PDI cylinders of length <100 nm can also be prepared by using lower m_{unimer}/m_{seed} ratios (see Figure S14).

ethanol, isopropanol (*i*-PrOH), *N*,*N*-dimethylformamide (DMF), dimethyl sulfoxide, and 1,4-dioxane at elevated temperatures followed by slowly cooling of the samples to room temperature and their subsequent aging for 2 days. However, spherical micelles or unimer films were formed, except in case of DMF, where coexistence of spheres, cylinders, and ill-defined 2D structures was observed (Figure S12). It is noteworthy that in the DMF sample, spheres were the predominant component. In an attempt to slow down the self-assembly process in DMF to promote accompanying core crystallization, slow evaporation of THF from the BCP solution in a mixture of DMF and THF (DMF:THF, 1:2) over a period of 1 week was studied (Figure 1a). As shown in the TEM micrograph in Figure 1b, this resulted in the formation of very long (>10 μm) cylindrical micelles. Interestingly, repeating this experiment in a mixture of H_2O and THF resulted in predominant formation of spheres in the presence of small number cylindrical micelles (Figure S11).

In order to investigate the crystallinity present in the PFS cores of the cylinders formed by the slow evaporation method, small- and wide-angle scattering (SAXS and WAXS) studies were performed on the assemblies in DMF (5 mg/mL). In the SAXS regime, isotropic scattering was detected (Figure S13a) and the intensity was analyzed using a previously described model for the scattering from a cylindrical core−shell micelle with a corona of decaying electron density.[75] This yielded a core radius of 3.65 nm and a corona thickness of 19.3 nm, similar values to those found in previous measurements on PFS-based cylindrical micelles.[76] WAXS analysis showed a Bragg reflection at 0.99 $Å^{-1}$, corresponding to a *d*-spacing of 6.3 Å, in good agreement with previous measurements.[75] This is ascribed to an interchain packing distance of 7.3 Å between parallel polymer chains (see Figure S13b and associated discussion). The mixed morphology sample prepared in a heating−cooling process was also studied by WAXS. A much weaker peak was detected in the data from this sample, indicating the presence of self-assembled materials with relatively lower crystallinity (Figure S13b).

2.3. Near Monodisperse Cylindrical Micelles of Linear-Brush BCP 4 by Living CDSA. Water-soluble PFS-based BCP micelles, including cylinders, have previously been reported by several methods.[77−80] However, no significant dimensional control was described and the samples were polydisperse. Furthermore, the BCPs utilized lacked functionalizable groups in the corona-forming block preventing facile modification of the micelle periphery with bioactive or imaging agents. As

DOI: 10.1021/jacs.5b13416
J. Am. Chem. Soc. 2016, 138, 4484−4493

Table 1. Contour Length Data for PFS-*b*-(PEO-*g*-TEG) Cylindrical Micelles in H_2O and DMF[a]

	m_{unimer}/m_{seed}[b]					
length data	2.5	5	10	15	20	30
L_n (nm)	167 (169)	240 (277)	449 (439)	583 (568)	741 (735)	1107 (1011)
L_w (nm)	177 (177)	253 (286)	461 (449)	604 (577)	763 (743)	1122 (1032)
L_w/L_n	1.05 (1.05)	1.06 (1.03)	1.03 (1.02)	1.03 (1.02)	1.03 (1.01)	1.01 (1.02)
σ/L_n	0.22 (0.22)	0.24 (0.18)	0.17 (0.15)	0.19 (0.12)	0.17 (0.10)	0.11 (0.14)

[a]Values are given in water and those in brackets correspond to data for the same sample of cylinders in DMF. [b]Data for seeds: L_n = 38 nm, L_w = 45 nm, L_w/L_n = 1.20, σ/L_n = 0.45.

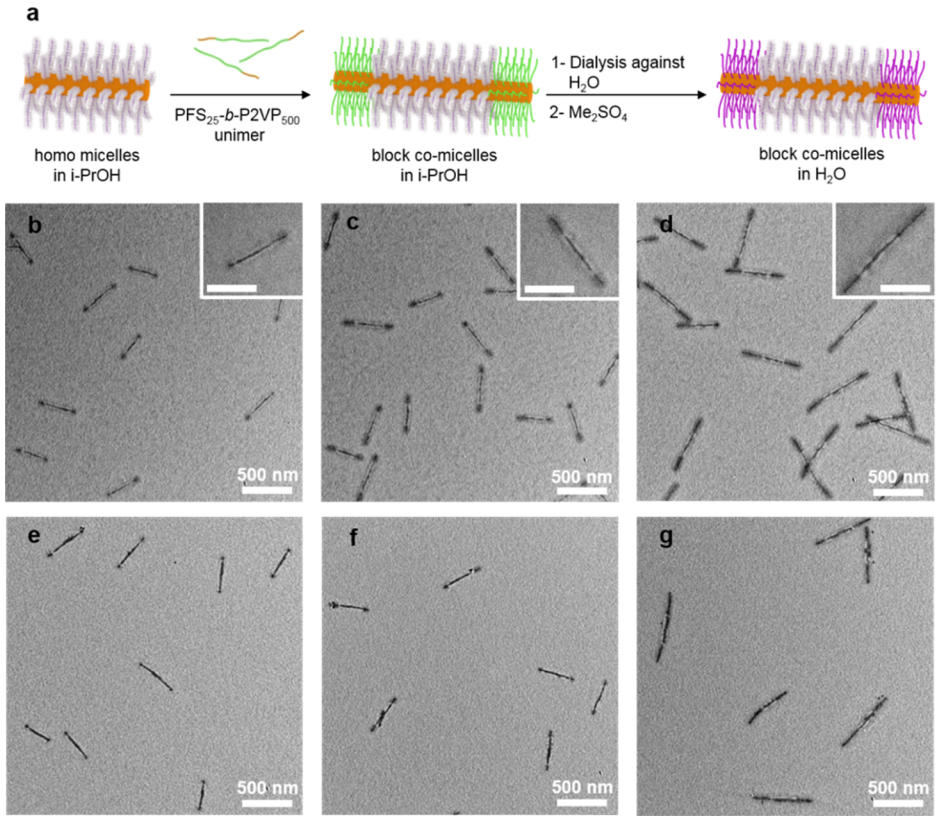

Figure 3. (a) Schematic representation of near monodisperse M(PFS_{25}-*b*-$P2VP_{500}$)-*b*-M(PFS-*b*-(PEO-*g*-TEG))-*b*-M(PFS_{25}-*b*-$P2VP_{500}$) triblock comicelles in *i*-PrOH and in water. Color coding of the coronas in the cartoons: gray (PFS-*b*-(PEO-*g*-TEG) cylinders), green (PFS_{25}-*b*-$P2VP_{500}$ blocks), and purple (quaternized PFS_{25}-*b*-$P2VP_{500}$ blocks). The PFS core is orange. TEM micrographs of triblock comicelles prepared by addition of 10 μg (b), 20 μg (c), and 40 μg (d) of PFS_{25}-*b*-$P2VP_{500}$ unimer to PFS-*b*-(PEO-*g*-TEG) cylinders (20 μg) in *i*-PrOH. Inset scale bars 250 nm. (e–g) TEM micrographs of triblock comicelles shown in (b–d) after quaternization in *i*-PrOH and subsequent dialysis against water.

discussed earlier, seeded growth methods associated with living CDSA have been shown to be a highly effective technique for the formation of near monodisperse micelles in organic and also in fluorinated media.[47,48] To apply this approach to linear-brush BCP **4**, a sample of long cylindrical micelles was sonicated with a sonotrode attached to a 50 W ultrasound processor at 0 °C for 30 min. This resulted in the formation of short seed crystallites (L_n = 38 nm, L_w = 45 nm, L_w/L_n = 1.20, σ/L_n = 0.45) (Figure 1c and d).

Cylindrical micelles of controlled length were obtained via the seeded growth approach (Figure 1a). To separate vials containing 10 μg of seed crystallites in DMF (0.05 mg/mL, 0.2 mL), different amounts of unimeric **4** as a 10 mg/mL solution in THF (25 μg, 50 μg, 100 μg, 150 μg, 200 μg, and 300 μg) were added and the resulting mixtures were aged for 2 days at room temperature (room temperature was consistently between 22 and 25 °C for all the experiments). TEM analysis of the samples revealed a linear relationship between the lengths of cylinders and the unimer-to-seed mass ratio (m_{unimer}/m_{seed}) (Figures S15–S21). It is noteworthy that L_n values obtained are in good agreement with the theoretical values indicating the formation of well-defined cylindrical micelles with quantitative addition of unimer to seeds. This resulted in the formation of cylindrical micelles up to 1.10 μm with narrow length distributions (L_w/L_n < 1.10) in DMF.

To lay the foundation for an exploration of the potential use of the near monodisperse cylindrical micelles in nanomedicine we targeted their dispersion in aqueous media. This was readily achieved via the simple dialysis of the cylinders formed in DMF against deionized (DI) water. As shown by TEM in Figure 2a–h and in the comparative data in Table 1, no significant change in the dimensions or polydispersities of the cylinders were detected utilizing this approach. Significantly, our group has previously shown that the cylindrical micelle length analysis data obtained from TEM imaging in dry state is in excellent agreement with that obtained from solution state techniques,

DOI: 10.1021/jacs.5b13416
J. Am. Chem. Soc. 2016, 138, 4484–4493

such as static light scattering and stimulated emission depletion microscopy and single molecule localization microscopy.[46,81] As a result, we believe that the data presented in Table 1 are a true reflection of the cylinder dimensions.

Having successfully prepared cylindrical micelles of controlled length in aqueous media, we also explored the possibility of performing seeded growth directly in water. To do this, cylindrical micelle seeds of **4** (L_n = 240 nm, L_w/L_n = 1.06) dispersed in DI water (0.027 mg/mL, 0.2 mL) were prepared and unimeric **4** (10 mg/mL, 2.7 μL) was added. After aging this sample for 4 days, subsequent analysis by TEM imaging revealed the presence of random populations of cylinders that did not undergo seeded growth, those grown from only one terminus, some unevenly grown from both termini, and new cylinders formed via spontaneous nucleation (Figure S22). Interestingly, the added segments to the seed cylinders in water exhibited significantly lower contrast by TEM compared to the central seed that was preformed in DMF. We believe that this may be a consequence of lower crystallinity (and hence density) of the PFS core formed directly in aqueous media due to rapid precipitation. Nevertheless, clearly the indirect dialysis method reported here is a viable approach to prepare cylindrical micelles of controlled dimension in aqueous media.

2.4. Water-Soluble B−A−B Multiblock Comicelles. Access to cylindrical multiblock comicelles with spatially segmented functionality in aqueous media is attractive for potential applications in biomedicine. To form such water-soluble cylindrical block comicelles, we initially investigated the formation of B−A−B amphiphilic structures in water-miscible organic media. In our design, the "A" block comprised the hydrophilic PFS-*b*-(PEO-*g*-TEG) BCP, and the "B" segments were based on the relatively more hydrophobic corona-forming block that could be subsequently transformed into a hydrophilic segment via a simple chemical transformation to allow water solubility. In addition, the amphiphilicity of such block comicelles prior to the transformation of the B blocks would allow their self-assembly behavior to be explored in aqueous media. This might result in the formation of cylindrical micelle-based superstructures[59,82] with potential applications in tissue engineering or as stimuli-responsive biomaterials.

To prepare the targeted B−A−B amphiphilic triblock comicelles with hydrophilic PFS-*b*-(PEO-*g*-TEG) as the "A" block, we selected PFS-*b*-P2VP (Figure S2) for growth of the relatively more hydrophobic "B" blocks via living CDSA (Figure 3a). The polar nature of the P2VP block would nevertheless allow the seeded growth process to be conducted in a polar organic medium in which the PFS-*b*-(PEO-*g*-TEG) seed cylinders are also soluble. In aqueous media, P2VP would be expected to act as a hydrophobic block and subsequent quaternization was therefore targeted as the method with which to impart hydrophilicity to these terminal block comicelle segments (Figure 3a).

To obtain the amphiphilic triblock comicelles, PFS-*b*-(PEO-*g*-TEG) cylinders in DMF were used as seeds to grow the PFS-*b*-P2VP blocks. The PFS_{25}-*b*-$P2VP_{500}$ hydrophobic terminal blocks were grown from PFS-*b*-(PEO-*g*-TEG) cylinders in DMF that was diluted with *i*-PrOH. We targeted the formation of triblock comicelles with three different lengths. Preformed PFS-*b*-(PEO-*g*-TEG) cylinders in DMF (L_n = 240 nm, L_w = 253 nm, L_w/L_n = 1.06, σ/L_n = 0.24, 20 μg) were dispersed in *i*-PrOH and PFS_{25}-*b*-$P2VP_{500}$ unimer in THF (10, 20, and 40 μg) was added. TEM analysis of the samples after aging for 24 h revealed the formation of well-defined triblock comicelles with short (L_n = 371 nm, L_w = 381 nm, L_w/L_n = 1.02, σ/L_n = 0.16), medium (L_n = 459 nm, L_w = 469 nm, L_w/L_n = 1.02, σ/L_n = 0.14), and long (L_n = 675 nm, L_w = 684 nm, L_w/L_n = 1.01, σ/L_n = 0.12) "B" blocks (Figure 3b−d and Figure S23−25). As shown in the TEM micrographs, the PFS_{25}-*b*-$P2VP_{500}$ blocks are easily distinguishable from the PFS-*b*-(PEO-*g*-TEG) block due to the inherent higher electron density of P2VP relative to the central PEO-*g*-TEG segment.

We envisioned that, depending on the length of the hydrophobic blocks, superstructures with different degrees of aggregation would form in an analogous manner to the well-characterized assemblies formed from amphiphilic block comicelles in organic media.[59] To test this hypothesis, DI water was first added dropwise (5-fold v/v relative to *i*-PrOH) to the well-defined triblock comicelles in *i*-PrOH and, after aging for 24 h, the resulting samples were dialyzed against DI water. Initial addition of water to the cylinders prior to dialysis was found to result in the formation of more colloidally stable hierarchical superstructures. As shown in Figure S26a, triblock comicelles with short hydrophobic segments self-assembled in one direction to form one-dimensional (1D) arrays of cylindrical micelles via end-to-end coupling of their hydrophobic blocks. On the other hand, with increasing length of the PFS_{25}-*b*-$P2VP_{500}$ segments, higher degrees of aggregation were observed (Figure S26b and c). We attribute the observed difference in the self-assembly behavior of these cylindrical micelles to the variation in their hydrophobic surface area. Thus, the hydrophobic surface area in cylindrical block comicelles with short terminal "B" segments of PFS_{25}-*b*-$P2VP_{500}$ is small, which favors only end-to-end coupling of the cylinders. In contrast, the corresponding surface area in the micelles with longer hydrophobic "B" segments is larger and therefore provides the opportunity for multiple block comicelles to self-organize around a single terminus.

As mentioned earlier, use of PFS_{25}-*b*-$P2VP_{500}$ to form the hydrophobic "B" segments offers the added advantage that P2VP quaternization should increase their hydrophilicity. This was investigated by treatment of the aforementioned B−A−B triblock comicelles superstructures with dimethyl sulfate (Me_2SO_4) in DI water. To ensure a high degree of quaternization (>80%), excess Me_2SO_4 was used (5.0 equiv relative to 2VP repeat units) (model experiments suggest a mixture of methylation (ca. 16%) and protonation (ca. 78%); see Figure S27 and associated text).[83] As shown in Figure 3e−g, upon addition of Me_2SO_4, subsequent aging of the samples for 24 h, and dialysis against DI water to remove excess Me_2SO_4, TEM analysis revealed complete disassembly of the superstructures and the formation of well-dispersed cylindrical block comicelles in aqueous media (for length and length distribution analysis of the water-soluble block comicelles see Figure S28−30 and Table 2).

More importantly, this provided a viable route to access multiblock comicelles in aqueous media, which has not been reported previously. This result is significant as it allows us to access cylindrical micelles with spatially segmented functionalities in aqueous media which, in turn, offers many potential applications in biomedical research.

2.5. DNA Immobilization by Triblock Comicelles. It has been shown that cationic polymers,[84] dendrimers,[85] liposomes,[86] and nanoparticles[87−89] can be used for DNA complexation via the interactions between their positively charged groups and DNA's negatively charged phosphate groups. This approach has been used in gene therapy for

DOI: 10.1021/jacs.5b13416
J. Am. Chem. Soc. 2016, 138, 4484−4493

Table 2. Contour Length Data for Cylindrical Triblock Comicelles in H_2O and *i*-PrOH[a]

	$m_{PFS\text{-}b\text{-}P2VP}/m_{PFS\text{-}b\text{-}(PEO\text{-}g\text{-}TEG)}$[b]		
length data	0.5	1	2
L_n (nm)	367 (371)	451 (459)	678 (675)
L_w (nm)	374 (381)	462 (469)	688 (684)
L_w/L_n	1.02 (1.02)	1.02 (1.02)	1.02 (1.01)
σ/L_n	0.14 (0.16)	0.16 (0.14)	0.12 (0.12)

[a]Values are given in water for the quaternized materials and those in brackets correspond to data for the same sample of cylinders (neutral) in *i*-PrOH. [b]Data for PFS-*b*-(PEO-*g*-TEG) seeds: L_n = 240 nm, L_w = 253 nm, L_w/L_n = 1.06, σ/L_n = 0.24.

successful protection of DNA from degradation.[90] To illustrate the biorelevance of our block comicelles with positively charged terminal segments, their ability to bind DNA was investigated (Figure 4a). The DNA strands used in this study were a commercially available native double-stranded DNA (purified from salmon testes, in its sodium salt form) containing ca. 2000 base pairs.

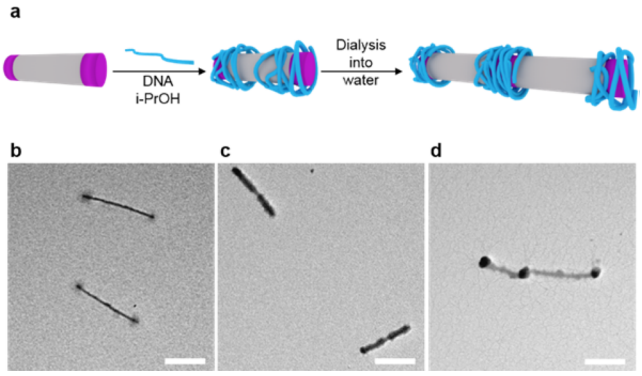

Figure 4. (a) Schematic representation of DNA interaction with quaternized triblock comicelles. TEM micrographs of (b) quaternized triblock comicelles in *i*-PrOH; (c) DNA-coated cylinders in *i*-PrOH; (d) DNA-coated cylinders after dialysis against DI water demonstrating "DNA glue" connecting cylinders end-to-end. Scale bars 250 nm.

First, triblock comicelles with short terminal PFS_{25}-*b*-$P2VP_{500}$ segments (Figure 3b), were quaternized in *i*-PrOH using Me_2SO_4 (5.0 equiv relative to 2VP repeat units) (Figure 4b) (model experiments suggest a mixture of methylation (ca. 66%) and protonation (ca. 26%); see Figure S27 and associated text). After dialysis against *i*-PrOH to remove excess Me_2SO_4, the interaction between the resulting cylindrical block comicelles and DNA (10-fold w/w relative to PFS_{25}-*b*-$P2VP_{500}$) was then investigated both in *i*-PrOH and water.

Interestingly, when *i*-PrOH was used as the solvent, this apparently resulted in nearly complete coating of the cylindrical micelles by DNA (Figure 4c and Figure S31). However, careful inspection of the TEM micrographs (e.g., Figure 4c) showed the central regions of the cylinders exhibited lower electron density, presumably due to the reduced localization of DNA. In principle, the attachment of DNA to the central PFS-*b*-(PEO-*g*-TEG) hydrophilic block is surprising as the surface positive charge necessary for electrostatic interactions with DNA is not present. Given the very limited solubility of DNA in *i*-PrOH, it is likely that the brush-type, TEG-covered surface of PFS-*b*-(PEO-*g*-TEG) middle block offers adequate hydrophilicity to the DNA strands, which in turn results in their deposition. It is also possible that the DNA strands initially interact with the positively charged terminal blocks of the cylinders and subsequently continue to cover the cylinders' surface toward the center of the micelle. To explore this further, in a control experiment, the DNA binding behavior of the seed cylinders (L_n = 240 nm, L_w/L_n = 1.02) from PFS-*b*-(PEO-*g*-TEG) used for the synthesis of triblock comicelles were investigated for DNA binding in *i*-PrOH. As shown in Figure S32, no detectable deposition of the DNA strands onto the surface was observed by TEM. Instead, DNA aggregates were formed in the solution. This indicated that the presence of positively charged terminal regions in the triblock comicelles are necessary to induce complexation and that the resulting deposition is not confined to these regions.

To access aqueous solutions of the DNA-coated cylindrical block comicelles, dialysis of the *i*-PrOH dispersions was performed against DI water. Upon the introduction of a good solvent for DNA, the strands detached from the central segment of the block comicelle. This resulted in the formation of DNA-cylinder network-type structures (Figure S33) and, in some cases, end-to-end and side-by-side coupling of the cylinders (Figure 4d and Figure S33).

The increased contrast in the terminal blocks of the block comicelles in Figure 4d compared to those shown in Figure 4a suggests that the DNA strands remain complexed to the quaternized P2VP corona in aqueous media. The binding of DNA to quaternized triblock comicelles was supported by zeta potential data. While the uncomplexed triblock cylinders showed a zeta potential value of 55.4 ± 2.4 mV in water, consistent with the presence of positively charged particles in solution, addition of DNA resulted this value to drop to −73.0 ± 1.6 mV. This decrease in the zeta potential value is consistent with coating the cationic segments of the cylinders with negatively charge DNA strands.

We attempted to gain more control in the formation of cylinder-DNA complex. This was partially achieved by the addition of 0.5 and 1 equiv (w/w relative to PFS_{25}-*b*-$P2VP_{500}$) of DNA to the positively charged triblock cylinders in aqueous media (L_n = 367 nm, L_w = 374 nm, L_w/L_n = 1.02). As shown in Figure S34, addition of 0.5 equiv of DNA (w/w relative to PFS_{25}-*b*-$P2VP_{500}$) resulted in the partial and random coating of the positively charged segments of the cylinders by DNA strands and a decrease in zeta potential to 31.7 ± 1.4 mV. On the other hand, by adding 1 equiv of DNA (w/w relative to PFS_{25}-*b*-$P2VP_{500}$) to the quaternized triblock comicelles in water, nearly all the positively charged blocks were complexed with DNA strands and, in a few instances, "gluing" of the cylinders was also observed (Figure 5 and Figure S35). This was accompanied by a further decrease in the zeta potential value to −32.4 ± 4.0 mV. These results suggest that, by optimizing complexation conditions, this system can potentially be explored as a DNA vector for gene therapy.

3. SUMMARY

We have developed a simple method for the preparation of near monodisperse cylindrical micelles of controlled length in aqueous media. In our approach, amphiphilic linear-brush PFS-*b*-(PEO-*g*-TEG) BCP was synthesized by a combination of anionic polymerization and photoinitiated thiol−ene "click" chemistry. PFS-*b*-(PEO-*g*-TEG) cylindrical micelles were prepared via living CDSA using a seeded growth approach in a wide length range up to 1.10 μm with low PDIs in DMF. Successful subsequent dispersion of these cylindrical micelles in

DOI: 10.1021/jacs.5b13416
J. Am. Chem. Soc. 2016, 138, 4484−4493

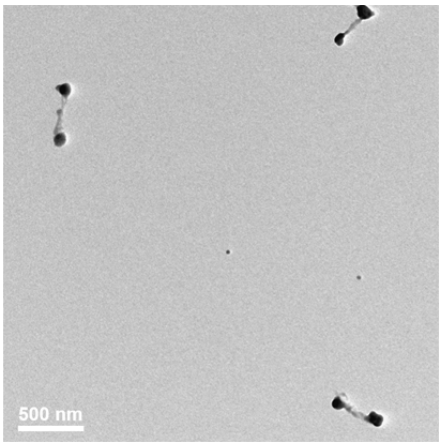

Figure 5. TEM micrograph showing near-complete coating of the positively charged terminal segments of quaternized triblock comicelles in DI water with DNA strands by adding 1 equiv (w/w relative to PFS_{25}-*b*-$P2VP_{500}$) of DNA to water-soluble triblock comicelles (L_n = 367 nm, L_w = 374 nm, L_w/L_n = 1.02).

aqueous media was accomplished by dialysis against DI water. Furthermore, B−A−B amphiphilic triblock comicelles using PFS-*b*-P2VP as the hydrophobic "B" block and PFS-*b*-(PEO-*g*-TEG) as the hydrophilic "A" block were constructed. Investigation of the hierarchical self-assembly behavior of the amphiphilic triblock comicelles in water showed the formation of superstructures with different degrees of aggregation. Subsequent quaternization of the PFS-*b*-P2VP segments using Me_2SO_4 in DI water resulted in the disassembly of the superstructures and formation of the first examples of well-defined triblock comicelles soluble in aqueous media.

To demonstrate the potential for this system in biomedical applications, triblock comicelles were used for the complexation of DNA. Interestingly, it was observed that in *i*-PrOH, DNA strands not only interact with the positively charged quaternized PFS-*b*-P2VP blocks, but also use it as the initiation point to interact and cover the neutral PFS-*b*-(PEO-*g*-TEG) segment. Dispersion of these structures in aqueous media, however, resulted in the detachment of DNA from the neutral segment and its selective complexation by the positively charged terminal blocks. These results, the possibility for surface functionalization through "click" reactions, and the flexibility and control permitted by living CDSA which allows access to near monodisperse and segmented micelle architectures, suggest that there is substantial potential for these types of cylindrical micelles in biomedicine. Detailed studies of in vitro cytotoxicity, cellular uptake, hydrogel formation, and the development of multifunctional cylindrical micelles that can also be used for imaging and therapeutic applications, are currently underway. In addition, the expansion of this approach that allows controlled access to near monodisperse cylindrical micelles and comicelles over a broad length range in aqueous media to analogous BCPs with crystallizable biodegradable cores represents an important target for the future.[39−44]

■ ASSOCIATED CONTENT

Supporting Information

The Supporting Information is available free of charge on the ACS Publications website at DOI: 10.1021/jacs.5b13416.

Experimental procedures and additional data. (PDF)

■ AUTHOR INFORMATION

Corresponding Author

*ian.manners@bristol.ac.uk

Notes

The authors declare no competing financial interest.

■ ACKNOWLEDGMENTS

A.N. is grateful to the European Union for a Marie Curie Fellowship. C.E.B. and D.J.L. thank the Bristol Chemical Synthesis Centre for Doctoral Training, funded by the Engineering and Physical Sciences Research Council, for PhD studentships. D.W.H. was supported by EPSRC doctoral training centre grant [EP/G036780/1]. M.A.W. thanks NSERC for support. I.M. is grateful to the EU for a European Research Council Advanced Investigator Grant. The Ganesha X-ray scattering apparatus used for this research was purchased under EPSRC Grant "Atoms to Applications" Grant ref EP/K035746/1. The authors are also grateful to Liam R. Macfarlane for the supply of P2VP homopolymer for NMR analysis.

■ REFERENCES

(1) Elsabahy, M.; Wooley, K. L. *Chem. Soc. Rev.* **2012**, *41*, 2545.
(2) Morachis, J. M.; Mahmoud, E. A.; Almutairi, A. *Pharmacol. Rev.* **2012**, *64*, 505.
(3) Such, G. K.; Yan, Y.; Johnston, A. P. R.; Gunawan, S. T.; Caruso, F. *Adv. Mater.* **2015**, *27*, 2278.
(4) Zhang, S.; Zhao, Y. *J. Am. Chem. Soc.* **2010**, *132*, 10642.
(5) Hayward, R. C.; Pochan, D. J. *Macromolecules* **2010**, *43*, 3577.
(6) Odian, G. *Principles of Polymerization*; John Wiley & Sons: New York, 2004.
(7) Schacher, F. H.; Rupar, P. A.; Manners, I. *Angew. Chem., Int. Ed.* **2012**, *51*, 7898.
(8) Zhang, L.; Eisenberg, A. *Science* **1995**, *268*, 1728.
(9) Zhong, S.; Cui, H.; Chen, Z.; Wooley, K. L.; Pochan, D. J. *Soft Matter* **2008**, *4*, 90.
(10) Pochan, D. J.; Chen, Z. Y.; Cui, H. G.; Hales, K.; Qi, K.; Wooley, K. L. *Science* **2004**, *306*, 94.
(11) Yan, D. Y.; Zhou, Y. F.; Hou, J. *Science* **2004**, *303*, 65.
(12) Koide, A.; Kishimura, A.; Osada, K.; Jang, W.-D.; Yamasaki, Y.; Kataoka, K. *J. Am. Chem. Soc.* **2006**, *128*, 5988.
(13) Zhang, J.; Liu, K.; Müllen, K.; Yin, M. *Chem. Commun.* **2015**, *51*, 11541.
(14) Xiong, X.-B.; Falamarzian, A.; Garg, S. M.; Lavasanifar, A. *J. Controlled Release* **2011**, *155*, 248.
(15) Shrestha, R.; Elsabahy, M.; Luehmann, H.; Samarajeewa, S.; Florez-Malaver, S.; Lee, N. S.; Welch, M. J.; Liu, Y.; Wooley, K. L. *J. Am. Chem. Soc.* **2012**, *134*, 17362.
(16) Sakurai, Y.; Kajimoto, K.; Hatakeyama, H.; Harashima, H. *Expert Opin. Drug Delivery* **2015**, *12*, 41.
(17) Geng, Y.; Dalhaimer, P.; Cai, S.; Tsai, R.; Tewari, M.; Minko, T.; Discher, D. E. *Nat. Nanotechnol.* **2007**, *2*, 249.
(18) Zhang, K.; Fang, H.; Chen, Z.; Taylor, J.-S. A.; Wooley, K. L. *Bioconjugate Chem.* **2008**, *19*, 1880.
(19) Zhang, K.; Rossin, R.; Hagooly, A.; Chen, Z.; Welch, M. J.; Wooley, K. L. *J. Polym. Sci., Part A: Polym. Chem.* **2008**, *46*, 7578.
(20) Huang, X.; Teng, X.; Chen, D.; Tang, F.; He, J. *Biomaterials* **2010**, *31*, 438.
(21) Doshi, N.; Prabhakarpandian, B.; Rea-Ramsey, A.; Pant, K.; Sundaram, S.; Mitragotri, S. *J. Controlled Release* **2010**, *146*, 196.
(22) Cheng, C.; Qi, K.; Germack, D. S.; Khoshdel, E.; Wooley, K. L. *Adv. Mater.* **2007**, *19*, 2830.
(23) Huang, K.; Rzayev, J. *J. Am. Chem. Soc.* **2009**, *131*, 6880.
(24) Li, Z.; Ma, J.; Lee, N. S.; Wooley, K. L. *J. Am. Chem. Soc.* **2011**, *133*, 1228.

DOI: 10.1021/jacs.5b13416
J. Am. Chem. Soc. 2016, 138, 4484−4493

(25) Rajaram, S.; Choi, T.-L.; Rolandi, M.; Fréchet, J. M. J. *J. Am. Chem. Soc.* **2007**, *129*, 9619.
(26) Kang, E.-H.; Lee, I. S.; Choi, T.-L. *J. Am. Chem. Soc.* **2011**, *133*, 11904.
(27) Mai, Y.; Eisenberg, A. *Chem. Soc. Rev.* **2012**, *41*, 5969.
(28) Qian, J.; Zhang, M.; Manners, I.; Winnik, M. A. *Trends Biotechnol.* **2010**, *28*, 84.
(29) Cao, L.; Manners, I.; Winnik, M. A. *Macromolecules* **2002**, *35*, 8258.
(30) Massey, J. A.; Temple, K.; Cao, L.; Rharbi, Y.; Raez, J.; Winnik, M. A.; Manners, I. *J. Am. Chem. Soc.* **2000**, *122*, 11577.
(31) Du, Z.-X.; Xu, J.-T.; Fan, Z.-Q. *Macromolecules* **2007**, *40*, 7633.
(32) Fairley, N.; Hoang, B.; Allen, C. *Biomacromolecules* **2008**, *9*, 2283.
(33) Fujiwara, T.; Miyamoto, M.; Kimura, Y.; Iwata, T.; Doi, Y. *Macromolecules* **2001**, *34*, 4043.
(34) Zhang, J.; Wang, L.-Q.; Wang, H.; Tu, K. *Biomacromolecules* **2006**, *7*, 2492.
(35) Schmalz, H.; Schmelz, J.; Drechsler, M.; Yuan, J.; Walther, A.; Schweimer, K.; Mihut, A. M. *Macromolecules* **2008**, *41*, 3235.
(36) Lazzari, M.; Scalarone, D.; Hoppe, C. E.; Vazquez-Vazquez, C.; Lòpez-Quintela, M. A. *Chem. Mater.* **2007**, *19*, 5818.
(37) Lee, E.; Hammer, B.; Kim, J.-K.; Page, Z.; Emrick, T.; Hayward, R. C. *J. Am. Chem. Soc.* **2011**, *133*, 10390.
(38) Qian, J.; Li, X.; Lunn, D. J.; Gwyther, J.; Hudson, Z. M.; Kynaston, E.; Rupar, P. A.; Winnik, M. A.; Manners, I. *J. Am. Chem. Soc.* **2014**, *136*, 4121.
(39) Kynaston, E. L.; Gould, O. E. C.; Gwyther, J.; Whittell, G. R.; Winnik, M. A.; Manners, I. *Macromol. Chem. Phys.* **2015**, *216*, 685.
(40) Petzetakis, N.; Dove, A. P.; O'Reilly, R. K. *Chem. Sci.* **2011**, *2*, 955.
(41) Petzetakis, N.; Walker, D.; Dove, A. P.; O'Reilly, R. K. *Soft Matter* **2012**, *8*, 7408.
(42) Sun, L.; Petzetakis, N.; Pitto-Barry, A.; Schiller, T. L.; Kirby, N.; Keddie, D. J.; Boyd, B. J.; O'Reilly, R. K.; Dove, A. P. *Macromolecules* **2013**, *46*, 9074.
(43) Pitto-Barry, A.; Kirby, N.; Dove, A. P.; O'Reilly, R. K. *Polym. Chem.* **2014**, *5*, 1427.
(44) Sun, L.; Pitto-Barry, A.; Kirby, N.; Schiller, T. L.; Sanchez, A. M.; Dyson, M. A.; Sloan, J.; Wilson, N. R.; O'Reilly, R. K.; Dove, A. P. *Nat. Commun.* **2014**, *5*, 5746.
(45) He, W.-N.; Zhou, B.; Xu, J.-T.; Du, B.-Y.; Fan, Z.-Q. *Macromolecules* **2012**, *45*, 9768.
(46) Wang, X.; Guerin, G.; Wang, H.; Wang, Y.; Manners, I.; Winnik, M. A. *Science* **2007**, *317*, 644.
(47) Hudson, Z. M.; Qian, J.; Boott, C. E.; Winnik, M. A.; Manners, I. *ACS Macro Lett.* **2015**, *4*, 187.
(48) Gilroy, J. B.; Gädt, T.; Whittell, G. R.; Chabanne, L.; Mitchels, J. M.; Richardson, R. M.; Winnik, M. A.; Manners, I. *Nat. Chem.* **2010**, *2*, 566.
(49) Schmelz, J.; Schedl, A. E.; Steinlein, C.; Manners, I.; Schmalz, H. *J. Am. Chem. Soc.* **2012**, *134*, 14217.
(50) Zhang, W.; Jin, W.; Fukushima, T.; Saeki, A.; Seki, S.; Aida, T. *Science* **2011**, *334*, 340.
(51) Ogi, S.; Sugiyasu, K.; Manna, S.; Samitsu, S.; Takeuchi, M. *Nat. Chem.* **2014**, *6*, 188.
(52) Ogi, S.; Stepanenko, V.; Sugiyasu, K.; Takeuchi, M.; Würthner, F. *J. Am. Chem. Soc.* **2015**, *137*, 3300.
(53) Pal, A.; Malakoutikhah, M.; Leonetti, G.; Tezcan, M.; Colomb-Delsuc, M.; Nguyen, V. D.; van der Gucht, J.; Otto, S. *Angew. Chem., Int. Ed.* **2015**, *54*, 7852.
(54) Robinson, M. E.; Lunn, D. J.; Nazemi, A.; Whittell, G. R.; De Cola, L.; Manners, I. *Chem. Commun.* **2015**, *51*, 15921.
(55) Kang, J.; Miyajima, D.; Mori, T.; Inoue, Y.; Itoh, Y.; Aida, T. *Science* **2015**, *347*, 646.
(56) Gädt, T.; Ieong, N. S.; Cambridge, G.; Winnik, M. A.; Manners, I. *Nat. Mater.* **2009**, *8*, 144.
(57) Rupar, P. A.; Chabanne, L.; Winnik, M. A.; Manners, I. *Science* **2012**, *337*, 559.
(58) Qiu, H.; Cambridge, G.; Winnik, M. A.; Manners, I. *J. Am. Chem. Soc.* **2013**, *135*, 12180.
(59) Qiu, H.; Hudson, Z. M.; Winnik, M. A.; Manners, I. *Science* **2015**, *347*, 1329.
(60) Jia, L.; Zhao, G.; Shi, W.; Coombs, N.; Gourevich, I.; Walker, G. C.; Guerin, G.; Manners, I.; Winnik, M. A. *Nat. Commun.* **2014**, *5*, 3882.
(61) Lee, B. F.; Kade, M. J.; Chute, J. A.; Gupta, N.; Campos, L. M.; Fredrickson, G. H.; Kramer, E. J.; Lynd, N. A.; Hawker, C. J. *J. Polym. Sci., Part A: Polym. Chem.* **2011**, *49*, 4498.
(62) Wurm, F.; Nieberle, J.; Frey, H. *Macromolecules* **2008**, *41*, 1909.
(63) Zhang, Y.; Lundberg, P.; Diether, M.; Porsch, C.; Janson, C.; Lynd, N. A.; Ducani, C.; Malkoch, M.; Malmström, E.; Hawker, C. J.; Nyström, A. M. *J. Mater. Chem. B* **2015**, *3*, 2472.
(64) Robb, M. J.; Connal, L. A.; Lee, B. F.; Lynd, N. A.; Hawker, C. J. *Polym. Chem.* **2012**, *3*, 1618.
(65) Dimitriou, M. D.; Zhou, Z.; Yoo, H.-S.; Killops, K. L.; Finlay, J. A.; Cone, G.; Sundaram, H. S.; Lynd, N. A.; Barteau, K. P.; Campos, L. M.; Fischer, D. A.; Callow, M. E.; Callow, J. A.; Ober, C. K.; Hawker, C. J.; Kramer, E. J. *Langmuir* **2011**, *27*, 13762.
(66) Hunt, J. N.; Feldman, K. E.; Lynd, N. A.; Deek, J.; Campos, L. M.; Spruell, J. M.; Hernandez, B. M.; Kramer, E. J.; Hawker, C. J. *Adv. Mater.* **2011**, *23*, 2327.
(67) Killops, K. L.; Gupta, N.; Dimitriou, M. D.; Lynd, N. A.; Jung, H.; Tran, H.; Bang, J.; Campos, L. M. *ACS Macro Lett.* **2012**, *1*, 758.
(68) Wang, R.; Hu, X.; Yue, J.; Zhang, W.; Cai, L.; Xie, Z.; Huang, Y.; Jing, X. *J. Mater. Chem. B* **2013**, *1*, 293.
(69) Barthel, M. J.; Rinkenauer, A. C.; Wagner, M.; Mansfeld, U.; Hoeppener, S.; Czaplewska, J. A.; Gottschaldt, M.; Träger, A.; Schacher, F. H.; Schubert, U. S. *Biomacromolecules* **2014**, *15*, 2426.
(70) Oh, S. S.; Lee, B. F.; Leibfarth, F. A.; Eisenstein, M.; Robb, M. J.; Lynd, N. A.; Hawker, C. J.; Soh, H. T. *J. Am. Chem. Soc.* **2014**, *136*, 15010.
(71) Barteau, K. P.; Wolffs, M.; Lynd, N. A.; Fredrickson, G. H.; Kramer, E. J.; Hawker, C. J. *Macromolecules* **2013**, *46*, 8988.
(72) Ni, Y.; Rulkens, R.; Manners, I. *J. Am. Chem. Soc.* **1996**, *118*, 4102.
(73) Lunn, D. J.; Boott, C. E.; Bass, K. E.; Shuttleworth, T. A.; McCreanor, N. G.; Papadouli, S.; Manners, I. *Macromol. Chem. Phys.* **2013**, *214*, 2813.
(74) Shen, L.; Wang, H.; Guerin, G.; Wu, C.; Manners, I.; Winnik, M. A. *Macromolecules* **2008**, *41*, 4380.
(75) Gilroy, J. B.; Rupar, P. A.; Whittell, G. R.; Chabanne, L.; Terrill, N. J.; Winnik, M. A.; Manners, I.; Richardson, R. M. *J. Am. Chem. Soc.* **2011**, *133*, 17056.
(76) Hayward, D. W.; Gilroy, J. B.; Rupar, P. A.; Chabanne, L.; Pizzey, C.; Winnik, M. A.; Whittell, G. R.; Manners, I.; Richardson, R. M. *Macromolecules* **2015**, *48*, 1579.
(77) Gohy, J. F.; Lohmeijer, B. G. G.; Alexeev, A.; Wang, X. S.; Manners, I.; Winnik, M. A.; Schubert, U. S. *Chem. - Eur. J.* **2004**, *10*, 4315.
(78) Wang, X. S.; Winnik, M. A.; Manners, I. *Macromolecules* **2005**, *38*, 1928.
(79) Natalello, A.; Alkan, A.; Friedel, A.; Lieberwirth, I.; Frey, H.; Wurm, F. R. *ACS Macro Lett.* **2013**, *2*, 313.
(80) For water-soluble vesicles see: Power-Billard, K. N.; Spontak, R. J.; Manners, I. *Angew. Chem., Int. Ed.* **2004**, *43*, 1260.
(81) Boott, C. E.; Laine, R. F.; Mahou, P.; Finnegan, J. R.; Leitao, E. M.; Webb, S. E. D.; Kaminski, C. F.; Manners, I. *Chem. - Eur. J.* **2015**, *21*, 18539.
(82) Qiu, H.; Russo, G.; Rupar, P. A.; Chabanne, L.; Winnik, M. A.; Manners, I. *Angew. Chem., Int. Ed.* **2012**, *51*, 11882.
(83) Yamaguchi, M.; Yamaguchi, Y.; Matsushita, Y.; Noda, I. *Polym. J.* **1990**, *22*, 1077.
(84) Son, S.; Kim, W. J. *Biomaterials* **2010**, *31*, 133.
(85) Zhou, J.; Wu, J.; Hafdi, N.; Behr, J.-P.; Erbacher, P.; Peng, L. *Chem. Commun.* **2006**, 2362.
(86) Geusens, B.; Lambert, J.; De Smedt, S. C.; Buyens, K.; Sanders, N. N.; Van Gele, M. *J. Controlled Release* **2009**, *133*, 214.

DOI: 10.1021/jacs.5b13416
J. Am. Chem. Soc. 2016, 138, 4484−4493

(87) Blum, J. S.; Saltzman, W. M. *J. Controlled Release* **2008**, *129*, 66.
(88) Zhang, K.; Jiang, M.; Chen, D. *Angew. Chem., Int. Ed.* **2012**, *51*, 8744.
(89) Zhang, K.; Miao, H.; Chen, D. *J. Am. Chem. Soc.* **2014**, *136*, 15933.
(90) Park, T. G.; Jeong, J. H.; Kim, S. W. *Adv. Drug Delivery Rev.* **2006**, *58*, 467.

DOI: 10.1021/jacs.5b13416
J. Am. Chem. Soc. 2016, 138, 4484−4493